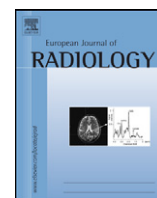




Since January 2020 Elsevier has created a COVID-19 resource centre with free information in English and Mandarin on the novel coronavirus COVID-19. The COVID-19 resource centre is hosted on Elsevier Connect, the company's public news and information website.

Elsevier hereby grants permission to make all its COVID-19-related research that is available on the COVID-19 resource centre - including this research content - immediately available in PubMed Central and other publicly funded repositories, such as the WHO COVID database with rights for unrestricted research re-use and analyses in any form or by any means with acknowledgement of the original source. These permissions are granted for free by Elsevier for as long as the COVID-19 resource centre remains active.



## Pneumonia in novel swine-origin influenza A (H1N1) virus infection: High-resolution CT findings

Ping Li<sup>a,\*</sup>, Dong-Ju Su<sup>b,\*\*</sup>, Ji-Feng Zhang<sup>a</sup>, Xu-Dong Xia<sup>a</sup>, Hong Sui<sup>c</sup>, Dong-Hui Zhao<sup>d</sup>

<sup>a</sup> Department of Radiology, The Second Affiliated Hospital of Harbin Medical University, 246 Xue Fu Road, Harbin 150086, China

<sup>b</sup> Department of Respiratory, The Second Affiliated Hospital of Harbin Medical University, 246 Xue Fu Road, Harbin 150086, China

<sup>c</sup> The Department of Statistics, Harbin Medical University, 240 Xue Fu Road, Harbin 150086, China

<sup>d</sup> Centers for Disease Control and Prevention of Heilongjiang, 187 Xiang An Street, Harbin 150036, China

### ARTICLE INFO

#### Article history:

Received 24 January 2010

Accepted 26 May 2010

#### Keywords:

CT

H1N1

Infectious diseases

Swine-origin influenza A

Pneumonia

### ABSTRACT

**Objective:** The purpose of our study was to review the initial high-resolution CT (HRCT) findings in pneumonia patients with presumed/laboratory-confirmed novel swine-origin influenza A (H1N1) virus (S-OIV) infection and detect pneumonia earlier.

**Materials and methods:** High-resolution CT (HRCT) findings of 106 patients with presumed/laboratory-confirmed novel S-OIV (H1N1) infection were reviewed. The 106 patients were divided into two groups according to the serious condition of the diseases. The pattern (consolidation, ground-glass, nodules, and reticulation), distribution, and extent of abnormality on the HRCT were evaluated in both groups. The dates of the onset of symptoms of the patients were recorded.

**Results:** The predominant CT findings in the patients at presentation were unilateral or bilateral multifocal asymmetric ground-glass opacities alone ( $n = 29$ , 27.4%), with unilateral or bilateral consolidation ( $n = 50$ , 47.2%). The consolidation had peribronchovascular and subpleural predominance. The areas of consolidation were found mainly in the posterior, middle and lower regions of the lungs. Reticular opacities were found in 6 cases of the initial MDCT scan. The extent of disease was greater in group 1 patients requiring advanced mechanical ventilation, with diffuse involvement in 19 patients (63.3%) of group 1 patients, and only 15/76 (19.7%) of group 2 patients ( $p < 0.01$ ,  $\chi^2$  test). 20 cases (19%) of the 106 patients had small bilateral or unilateral pleural effusions. None had evidence of hilar or mediastinal lymph node enlargement on CT performed at admission or later.

**Conclusions:** The most common radiographic and CT findings in patients with S-OIV infection are unilateral or bilateral ground-glass opacities with or without associated focal or multifocal areas of consolidation. On HRCT, the ground-glass opacities had a predominant peribronchovascular and subpleural distribution. CT plays an important role in the early recognition of severe S-OIV (H1N1).

© 2010 Elsevier Ireland Ltd. All rights reserved.

### 1. Introduction

During the spring of 2009, a novel swine-origin influenza A (H1N1) virus (S-OIV) was first reported in Mexico and spread globally [1]. The World Health Organization declared the first phase 6 global influenza pandemic of the century on June 11, 2009. During peak periods of seasonal influenza, the pandemic strain of H1N1 virus caused severe illness, including pneumonia, acute respiratory distress syndrome (ARDS) and even death. Antiviral drugs were administered to most patients, but such therapy was started more than 48 h after the onset of illness in a majority of the patients.

Delayed initiation of antiviral therapy may have contributed to an increased severity of illness [2]. It is therefore important that clinicians and radiologists be able to recognize chest CT findings of H1N1 influenza in high-risk groups so that they order specific antiviral therapy as soon as possible, especially in the countryside without appropriate diagnostic tests to confirm the diseases [3]. Multi-slice CT (MSCT) is the best technique to detect the early pneumonia compared with other techniques. In this article, we review initial HRCT findings characteristics of 106 patients who were hospitalized for pneumonia with presumed/laboratory-confirmed novel S-OIV (H1N1) in order to detect pneumonia with H1N1 earlier.

### 2. Materials and methods

#### 2.1. Subjects

We collected 106 patients hospitalized for pneumonia with presumed/laboratory-confirmed novel S-OIV (H1N1) infection

\* Corresponding author. Tel.: +86 0451 86605576; fax: +86 0451 86605408.

\*\* Corresponding author.

E-mail addresses: [pinglee.2000@yahoo.com](mailto:pinglee.2000@yahoo.com), [pinglee.2000@sina.com](mailto:pinglee.2000@sina.com) (P. Li),

[hyd.sdj@yahoo.com.cn](mailto:hyd.sdj@yahoo.com.cn) (D.-J. Su), [zjf2005520@163.com](mailto:zjf2005520@163.com) (J.-F. Zhang),

[xiaxd888@163.com](mailto:xiaxd888@163.com) (X.-D. Xia), [suisuihong@126.com](mailto:suisuihong@126.com) (H. Sui),

[yhw00000@yahoo.com.cn](mailto:yhw00000@yahoo.com.cn) (D.-H. Zhao).

**Table 1**  
Distribution of the disease in the two groups.

	Distribution		Predominant distribution		
	Bilateral	Unilateral	Central	Subpleural	Central and subpleural
Group 1 (n = 30)	15	60	19	30	26
Group 2 (n = 76)	1	30	3	6	22
Total	16	90	22	36	48

p > 0.05.

from October 2009 to December 2009. Our study group of patients included 54 males and 52 female ranging in age from 1 to 71 years (median age, 31.7 ± 15.7 years). 102 of the 106 patients had no significant medical history. 38 of these patients were confirmed to have S-OIV (H1N1) by testing of respiratory specimens with real-time reverse transcription polymerase chain reaction (RT-PCR) at Centers for Disease Control and Prevention (CDC). A confirmed case was defined by a positive result of a RT-PCR of nasal swabs or aspirates performed at a laboratory operated according to the guidelines of the Chinese Center for Disease Control and Prevention. The others were presumed to have S-OIV (H1N1) based on the fact that no other viruses were circulating in the community at any frequency. A suspected case was defined as an influenza-like illness (temperature ≥ 37.5 °C and at least one of the following symptoms: sore throat, cough, rhinorrhea, or nasal congestion) and either a history of travel to a country where infection had been reported in the

previous 7 days or an epidemiologic link to a person with confirmed or suspected infection in the previous 7 days [4]. All 106 patients had initially presented with an influenza-like illness, thereby fulfilling the clinical criteria for diagnosing S-OIV infection as established by the CDC. The bacterial or fungus cultures obtained within 24 h after admission were negative: cultures of blood specimens and bronchial aspirate samples from all patients.

The 106 patients were divided into two groups. Group 1 consisted of 30 critically ill patients. Critically ill patients were defined as (1) those admitted to a intensive care unit (ICU) or those requiring mechanical ventilation (invasive or noninvasive), (2) those with a fraction of inspired oxygen (FIO<sub>2</sub>) concentration greater than or equal to 60%, or (3) those with the need for intravenous infusion of inotropic or vasopressor medication [5]. Group 2 consisted of 76 patients who were required brief hospitalization without advanced mechanical ventilation but drugs.

All 106 patients were performed CT scans (some also with radio-graphy) and abnormal findings can be detected. Some critically ill

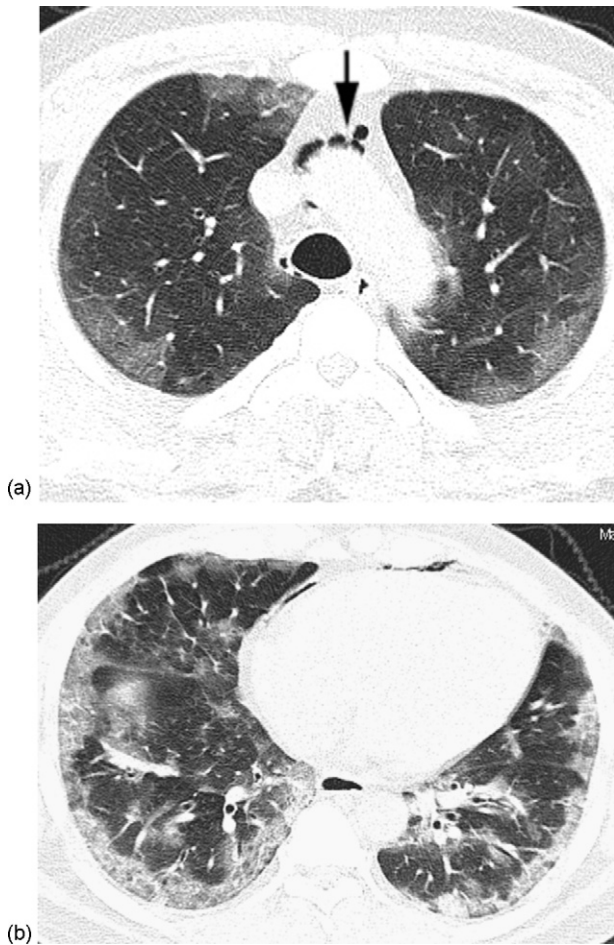


**Fig. 1.** A 36-year-old man with laboratory-confirmed S-OIV (H1N1). High-resolution CT (HRCT) scan obtained 10 days after the onset of symptoms. Axial CT image showed peripheral and lower lung predominant ground-glass opacities, and pneumomediastinum (arrows) (A and B).

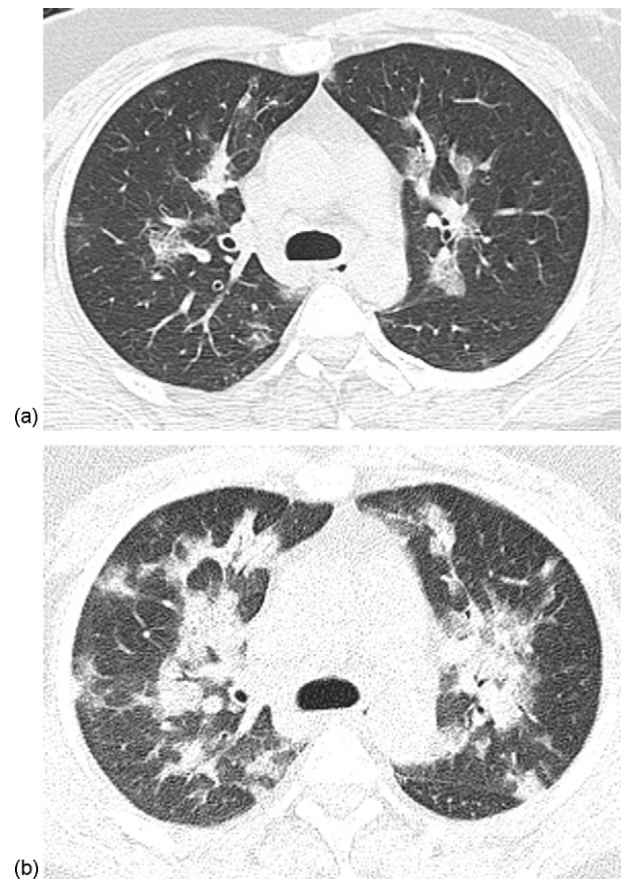


**Fig. 2.** A 34-year-old pregnant woman with laboratory-confirmed S-OIV (H1N1). High-resolution CT (HRCT) scan obtained on the day of the onset of fever (A). Axial CT image showed ground-glass opacities peribronchovascular and subpleural predominance. 3 days later, the opacities became larger and thicker on the same level as A (B).

patients confirmed H1N1 without CT scans in our hospital were not included in this study.

## 2.2. Imaging techniques

Thin-section MSCT was performed in all 106 patients. 80 patients underwent MDCT on admission, whereas the remaining patient underwent scanning within 24 h after admission. 72 of the 80 patients had second MDCT scan 14 days after the initial study. 26 patients underwent initial CT in other hospital and second MDCT in our hospital. The other patients had no CT scans but bedside anteroposterior-projection radiographs because their serious condition. The studies were performed on a 10-MDCT scanner (Sensation10, Siemens Healthcare) or 16-MCT scanner (lightspeed 16, GE Healthcare). The protocol used was as follows: end-inspiratory acquisition, 120 kV, 150–200 mAs, and 2-mm reformation. The images were viewed on both lung (window width, 1400 HU; level, –700 HU) and mediastinal (window width, 350 HU; level, 40 HU) settings. The reconstructions were made in 2 mm-slice-thick and lung settings. 26 of the initial CT scans were obtained using a variety of CT scanners and protocols at other hospitals before the patients were transferred to our hospital. All 30 patients in ICU had serial bedside anteroposterior-projection follow-up radiographs. Initial chest radiographs were obtained using computed radiography or digital radiography in all patients.

## 2.3. Image analysis

Two experienced radiologists with thoracic imaging experience of 12 years and 14 years reviewed MDCT scans independently and reached a decision on the final interpretations by consensus. The abnormalities were further characterized as consolidation, ground-glass opacity, nodules, and reticulation. Ground-glass opacities were defined as hazy areas of increased opacity or attenuation without obscuration of the underlying vessels. Consolidation was defined as homogeneous opacification of the parenchyma with obscuration of the underlying vessels. Nodular opacities were defined as focal round opacities. Reticular opacities were defined as linear opacities forming a meshlike pattern. The involvement was categorized as unilateral or bilateral. If the involvement was deemed bilateral, the process was categorized as symmetric or asymmetric in nature. The distribution was categorized as focal, multifocal, and diffuse. Focal was defined as a single focus of abnormality, multifocal as more than one focus, and diffuse if bilateral and involving the equivalent of the volume of one or both lungs. Predominant distribution was also assessed as being in the upper, middle, or lower lung zone and as being in a random, predominantly central or peribronchovascular, or peripheral (outer third of the lungs) location. The presence of associated hilar, mediastinal lymph node enlargement, or pleural abnormalities was also assessed. Any additional lung findings were recorded. To assess changes that occurred over time, the CT scans in some patient were examined in sequence. The pattern, extent, and distribution of abnormal CT findings were compared with findings in the same region on previous and subsequent CT scans. The date of the onset of symptoms and the date of the earliest CT scans of all the patients were recorded. We evaluated the interval days that between the onset of the symptom and the initial CT scans.

## 2.4. Statistical analysis

For categorical variables, the percentages of patients in each category were calculated.  $p < 0.05$  was considered to indicate a statistically significant difference. Differences in the two groups were

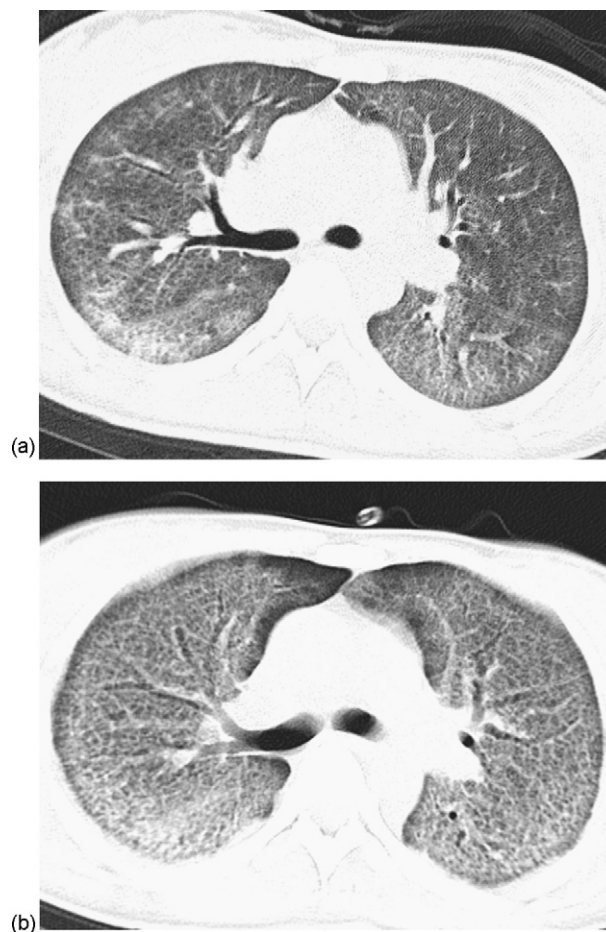


**Fig. 3.** A 36-year-old woman with laboratory-confirmed S-OIV (H1N1). Chest CT acquired at admission showed bilateral ground-glass opacities in all lung zones (A) and reticular opacities in right lower lobe. Follow-up CT performed 12 days after A showed follow-up CT reticular opacities forming a meshlike pattern (B).

tested by using  $\chi^2$  statistics. All of the data were analyzed with statistical software (SPSS, version 13.0; SPSS, Chicago, IL).

## 3. Results

There were 30 critically ill patients admitted to the ICU requiring intubation or mechanical ventilation. There is no difference between the age of the two groups ( $p < 0.05$ ). None of our patients with H1N1 had normal CT findings at presentation. The HRCT findings at presentation in our patients were similar to those described by the reports [6]. The predominant radiographic findings in the patients at presentation were unilateral or bilateral multifocal asymmetric ground-glass opacities alone ( $n = 29$ , 27.4%), with unilateral or bilateral consolidation ( $n = 50$ , 49.2%), nodular opacities or reticular opacities (Table 1). The initial MDCT scan displayed a pattern of rounded, multiple, peripheral ill-defined ground-glass opacities, including two patients who are pregnant (Figs. 1 and 2). The sharp demarcation between the areas of involved and uninvolved parenchyma can be seen on CT scans. The consolidation had peribronchovascular and subpleural predominance. The areas of consolidation were found mainly in the posterior, middle and lower regions of the lungs, but there was no difference between the two groups (Table 1). Reticular opacities were found in 6 cases of the initial MDCT scan (Fig. 3). There was no difference between the pattern of disease of the two groups (Table 2). Thickening of interlobular septa and intralobular lines in both sides can be seen (Fig. 4). 30 cases (31%) of the 106 patients who were hospitalized

**Table 2**

The patterns of the disease in the two groups.

	Ground-glass opacities	Consolidation	Nodular opacities	Reticular opacities
Group 1 (n = 30)	20	29	3	2
Group 2 (n = 76)	59	48	1	13
Total (n = 106)	79	77	4	15

 $p > 0.05$ .**Table 3**

Distribution of the disease in the two groups.

	Distribution			Predominant distribution		
	Focal	Multifocal	Diffuse	Upper lung zone	Middle lung zone	Lower lung zone
Group 1 (n = 30)	1	10	19	8	29	30
Group 2 (n = 76)	9	52	15	40	56	72
Total (n = 106)	10	62	34	48	85	102

 $p < 0.001$ .

and had follow-up CT and obtained within 24 h of presentation showed progression of the disease (Fig. 5). The most outstanding CT features of the disease include rapidly-progressing basal and axial interstitial/alveolar consolidation and diffuse ground-glass opacities (Fig. 5C). The extent of disease was greater in group 1 patients requiring advanced mechanical ventilation, with diffuse involvement in 19 patients (63.3%) of group 1 patients, and only 15/76 (19.7%) of group 2 patients ( $p < 0.001$ ,  $\chi^2$  test) (Table 3). The one patient in group 1 who had focal disease involving only unilateral lower zones was admitted to ICU for dyspnea and died after 2 days. On CT scans, swelling of brain stem and bilateral thalamus were found (Fig. 6). There are 4 patients with pneumomediastinum in both groups that were only evident on high-resolution CT (Fig. 1). 20 cases (19%) of the 106 patients had small bilateral or unilateral pleural effusions. Pleural effusions decreased gradually on follow-up. None had evidence of hilar or mediastinal lymph node enlargement on CT performed at admission or later.

#### 4. Discussion

Swine influenza is a highly contagious acute respiratory disease of pigs caused by a subtype of influenza A virus. The modes of transmission of influenza viruses in humans, including S-OIV, are thought to occur mainly through the dissemination of large droplets and possibly small-particle droplet expelled when an infected person coughs [7,8]. The most common clinical findings

at presentation are fever, cough, dyspnea, and respiratory distress [7]. Although most cases of swine-origin influenza A (H1N1) virus (S-OIV) have been self-limited, fatal cases raise questions about virulence and radiology's role in early detection. Frequently reported complications of H1N1 influenza have included pneumonia, bacterial coinfection, acute necrotizing encephalopathy (ANE) and exacerbation of underlying medical conditions, such as congestive heart failure. The majority of fatal outcomes in the United States have been related to pulmonary complications [9,10].

The patients described were part of an epidemic of influenza-like illness with pneumonia seen at our hospitals, and only a part of them (38 cases, 35.8%) tested positive for S-OIV. A false negative test in patients who had infection with S-OIV would be more likely if the test were delayed or if patients had limited viral shedding [2]. The result of a RT-PCR of nasal swabs or aspirates of our 38 confirmed cases became negative during the follow-up. The negative results of the follow-up RT-PCR of nasal swabs suggested that the test were delayed for various reasons.

H1N1 influenza is still a novel disease with poorly understood pathology and pathogenesis. The histologic changes of pneumonia in H1N1 are characteristics of influenza though not pathognomonic. Autopsies have shown that the main pathological changes associated with S-OIV infection are localized to the lungs [11]. The lungs typically show diffuse alveolar damage (DAD) [12]. In the early phase of the disease (<10 to 12 days), features of the exudative inflammatory phase of diffuse alveolar damage are predominant. There are hyaline membranes, alveolar septal edema, hyperplasia of type II pneumocytes and fibrin thrombus in the vascular lumen. That is corresponding with ground-glass opacities and consolidations on CT scans. The following additional histopathological features have also been reported: inflammatory infiltrate below the endothelium and partial loss and adherence of the endothelium in intrapulmonary blood vessels; pneumonia foci with intraalveolar exudates without evidence of bacterial colonies [12]; necrotizing bronchiolitis [11]; extensive hemorrhage [11]; pleuritis; interstitial pneumonitis; cytopathic effect in the bronchial and alveolar epithelial cells and epithelial hyperplasia and squamous metaplasia of the large airways [13]. In cases with longer disease duration, changes consistent with the fibrous proliferative phase (organizing diffuse alveolar damage) and the final fibrotic stage (interstitial fibrosis) have been observed [14]. One contributing factor for death in our patients may have been delayed admission and delayed initiation of oseltamivir or mechanical ventilation. Possible mechanisms of damage include direct injury to the respiratory epithelium with a secondary cytokine storm [2].



**Fig. 4.** A 39-year-old woman with presumed H1N1. High-resolution CT scan obtained on 3 days after the onset of symptoms showed ground-glass opacities, thickening of interlobular septa (arrows) and intralobular lines in both sides.

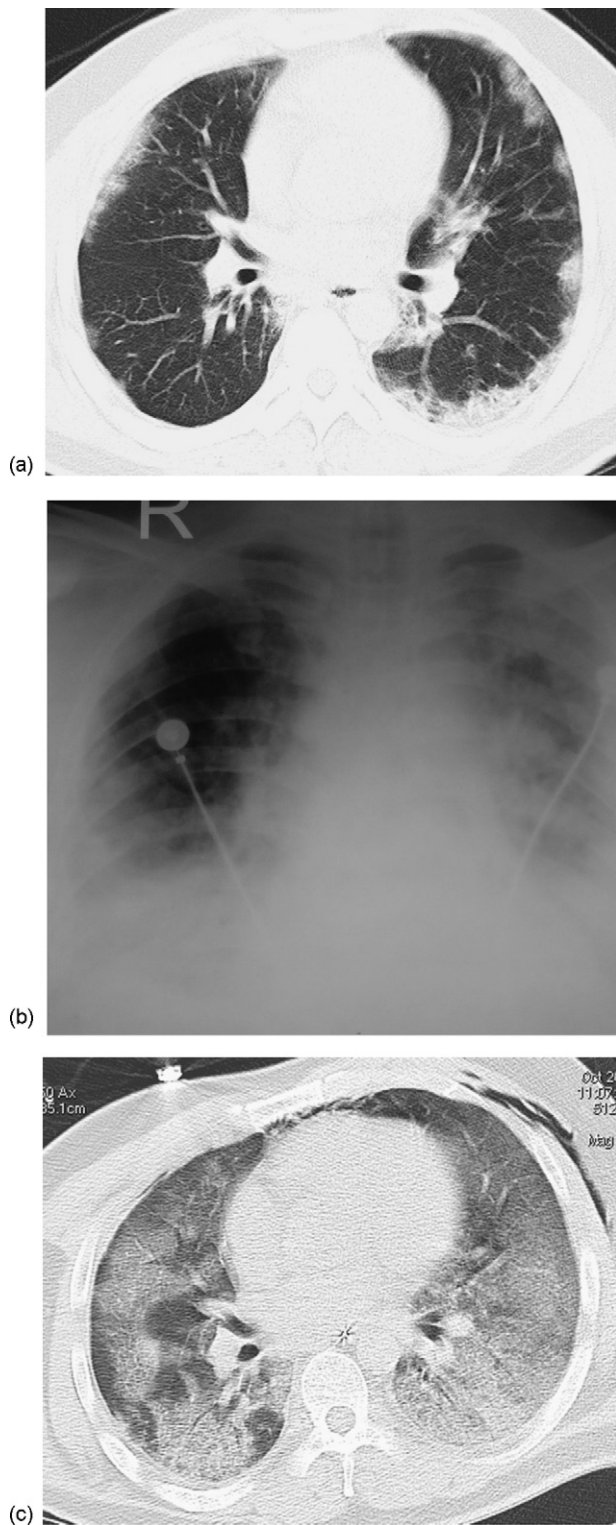


**Fig. 5.** A 34-year-old man with laboratory-confirmed S-OIV (H1N1). Chest CT acquired at admission (3 days after symptom onset) showed a peripheral distribution of patchy ground-glass opacities (A). With progression of the symptoms, chest radiograph obtained 2 days after hospital admission (B) showed bilateral areas of consolidation in mid and lower lung zones. He was admitted to ICU on the same day for mechanical ventilation. The ground-glass opacities were located throughout the upper and lower regions of all lobes in a peribronchovascular distribution. CT scan obtained on the third days after A (C) showed diffuse bilateral ground-glass opacities, areas of consolidation predominately in subpleural and dependent lung regions.

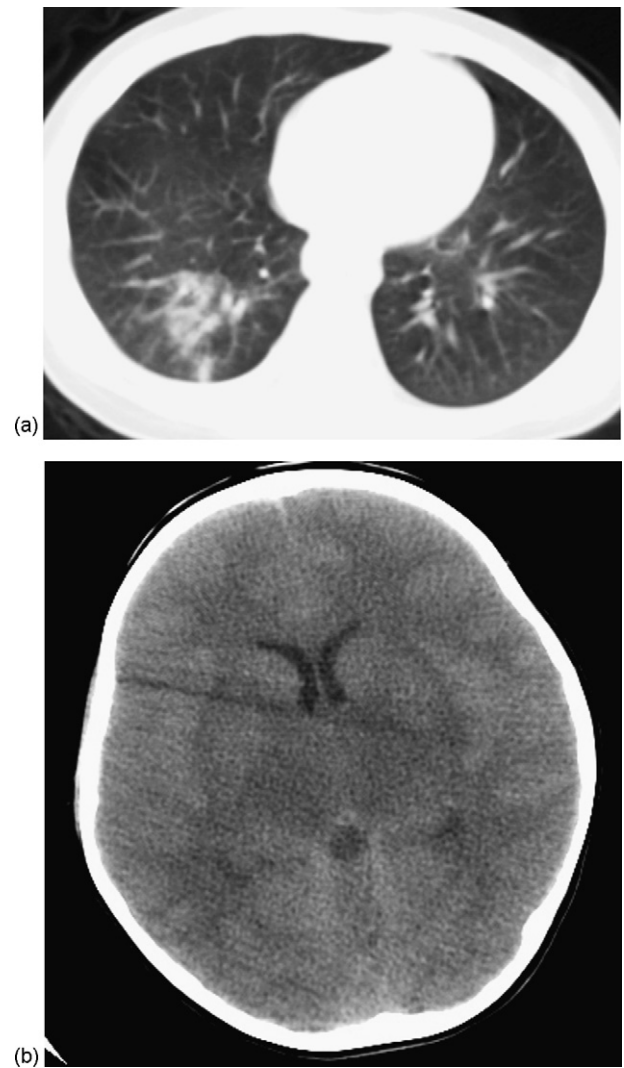


**Fig. 6.** A 5-year-old girl with laboratory-confirmed S-OIV (H1N1). Chest CT scan obtained 6 h after the onset of fever showed focal ground-glass opacities in right lower lobe (A). Head CT acquired on the same day with A showed swelling and the decreases cerebral stem and bilateral thalamus (B). She was admitted to ICU for mechanical ventilation immediately. She died on third hospital day.

Because the above histopathological features H1N1 influenza are not unique, it may be difficult to distinguish diffuse alveolar damage caused by H1N1 virus infections from diffuse alveolar damage caused by other microorganisms such as severe acute respiratory syndrome (SARS) coronavirus (SARS-CoV) or avian influenza A (H5N1) influenza [11]. So the CT findings of pneumonia in H1N1 were similar to that in SARS.

Typical initial CT findings of our patients showed bilateral multifocal asymmetric ground-glass opacities and consolidation in predominant subpleural and peribronchovascular distribution—corroborate those in previous preliminary reports [15,16]. However, ground-glass opacities were by far the most common finding in our patients, being more commonly bilateral than unilateral. Another observation in our patients was that the progression of radiographic abnormalities was mostly in the form of developing multifocal areas of consolidation on follow-up.

HRCT was superior to radiography in showing the distribution extensive involvement of the disease. An interesting observation on the HRCT scans was the distinctive peribronchovascular and peripheral distribution of the disease. This appearance is similar to that seen in cases of organizing pneumonia. The similarity of typi-

cal CT findings in cases of S-OIV and in cases of early severe acute respiratory syndrome (SARS) has been previously raised [17,18]. We also noted that similarity in our group of patients. During the initial phases of both diseases the virus cause exudative inflammatory alveolar and interstitial edema that result in both MDCT finding dominated by ground-glass opacities (GGO) [18]. Severe cases can develop radiologic and pathologic findings of diffuse alveolar damage rapidly and the patients present with hemoptysis, even acute respiratory distress syndrome (ARDS) [19]. In addition, both diseases showed no centrilobular nodules, tree-in-bud pattern, cavity, pleural effusion, or mediastinal or hilar lymphadenopathy [20]. However, 19% of the patients with pleural effusion were found in our group of patients. The absence of centrilobular and tree-in-bud opacities further decreases the suggestion of bronchiolitis and small-airway inflammation at the level of the secondary lobule. Radiologic recovery from H1N1 can be complete, but computed tomography images often show persistent GGO and reticular opacities, some of which reflect pathologic findings of fibrosis. Long-term follow-up imaging of survivors shows gradual decrease of GGO and reticulation with persistent air trapping in some patients. The latter is evidence of small-airway disease that cannot be detected on CT scans at the onset of the disease [19].

Characterization as ground-glass opacities are generally pathologically attributable to the partial displacement of air from partial filling of air spaces, thickening of interstitial tissues from fluid or cells, partial alveolar collapse, or increased capillary blood volume [3,21]. The imaging findings in this case, therefore, suggest a differential diagnosis of atypical infection (including viral infection; *Mycoplasma*, *Chlamydia*, or *Legionella* infection; and septic emboli), ARDS, cryptogenic organizing pneumonia (COP), eosinophilic pneumonitis, and hypersensitivity pneumonitis [22].

Although most patients with HRCT abnormalities can be showed on the corresponding chest radiographs, however, the extent of involvement was more diffuse and the distribution of disease was better characterized on MDCT [16].

The University of Michigan series reports a high incidence of pulmonary emboli among its most severely affected patients, especially in obesity. An association of viral infection and thromboembolic disease has been questioned on occasion, including with SARS, but is not common [18]. It is possible that the causal association is between obesity and severe S-OIV infection, and the increased rate of thromboembolic disease may be related to obesity. None of the patients in our study underwent lung biopsy or autopsy that would have allowed radiographic–histopathologic correlation. None of the patients in our study underwent contrast enhancement to exclude the embolism of pulmonary embolism (PE).

Patients who are hospitalized with suspected influenza and lung infiltrates on chest radiography should be considered for treatment with both antibiotics and antiviral drugs. Early treatment with neuraminidase inhibitors (oseltamivir or zanamivir) is ideal and may help patients with severe illness. Jain [2] suggests that the use of antiviral drugs is beneficial, especially in early state, since patients who were admitted to an ICU or died were less likely to have received such therapy within 48 h after the onset of symptoms. The time from hospitalization to the need for mechanical ventilation might be as short as 24 h or less [1]. Some patients developed severe acute respiratory distress syndrome (ARDS) and were treated with extracorporeal membrane oxygenation (ECMO) [2,23]. CT findings manifest as extensive bilateral air-space disease in hospitalized patients requiring advanced mechanical ventilation.

Our study has several limitations. The patients we evaluated represented 80% of total hospitalizations in our hospital for 2009 H1N1 infection that were reported to the CDC during October 2009 to December 2009. We evaluated pneumonia patients with presumed/confirmed H1N1 who had CT scans, so the group may not

be representative of hospitalized patients who may not have been tested. Despite the use of a standardized data-collection form, not all information was collected for all patients. The further research to assess the effect of treatment will be evaluated by follow-up CT.

In conclusion, the most common radiographic and MDCT findings in patients with S-OIV infection are unilateral or bilateral ground-glass opacities with or without associated focal or multifocal areas of consolidation. These imaging findings raised suspicion of S-OIV despite negative H1N1 influenza rapid antigen test results from two nasopharyngeal swabs; subsequently, those results were proven to be false-negatives by reverse transcriptase polymerase chain reaction. This suggests a role for CT in the early recognition of severe S-OIV.

## Funding

Supported by grants from the National Science and Technology Projects (2007C30700189).

## Conflict of interest

No potential conflict of interest relevant to this article was reported.

## Acknowledgements

We thank Drs. Yong Wan, Deli Zhao, Dan Wang, Hongliang Wang Changzhen wang and Guanzhi Wang for their help with the collection of clinical data; Dr. Lijuan Zhang, for their careful editing of an earlier version of this article; and Dr. Yanming Zhao for technical support.

## References

- [1] Perez-Padilla R, de la Rosa-Zamboni D, Ponce de Leon S, et al. Pneumonia and respiratory failure from swine origin influenza A (H1N1) in Mexico. *N Engl J Med* 2009;361(7):680–9.
- [2] Jain S, Kamimoto L, Bramley AM, et al. Hospitalized patients with 2009 H1N1 influenza in the United States, 2009. *N Engl J Med* 2009;20(361):1935–44.
- [3] Mollura DJ, Asnis DS, Crupi RS, et al. Imaging findings in a fatal case of pandemic swine-origin influenza A (H1N1). *AJR* 2009;193(6):1500–3.
- [4] Cao B, Li XW, Mao Y, et al. Clinical features of the initial cases of 2009 pandemic influenza A (H1N1) virus infection in China. *N Engl J Med* 2009;361(26):680–9.
- [5] Kumar A, Zarychanski R, Pinto R, et al. Critically ill patients with 2009 influenza A (H1N1) infection in Canada. *JAMA* 2009;302(17):1872–9.
- [6] Agarwal PP, Cinti S, Kazerooni EA. Chest radiographic and CT findings in novel swine-origin influenza A (H1N1) virus (S-OIV) infection. *AJR* 2009;193(6):1488–93.
- [7] Dawood FS, Jain S, Finelli L, et al. Emergence of a novel swine-origin influenza A (H1N1) virus in humans. *N Engl J Med* 2009;360(25):2605–15.
- [8] Neumann G, Noda T, Kawaoka Y. Emergence and pandemic potential of swine-origin H1N1 influenza virus. *Nature* 2009;459(7249):931–9.
- [9] Thompson WW, Shay DK, Weintraub E, et al. Influenza-associated hospitalizations in the United States. *JAMA* 2004;292(11):1333–40.
- [10] Harper SA, Bradley JS, Englund JA, et al. Seasonal influenza in adults and children – diagnosis, treatment, chemoprophylaxis, and institutional outbreak management: clinical practice guidelines of the infectious diseases society of America. *Clin Infect Dis* 2009;48(8):1003–32.
- [11] Maud T, Hajjar LA, Callegari GD, et al. Lung pathology in fatal novel human influenza A (H1N1) infection. *Am J Respir Crit Care Med* 2010;181(1):72–9.
- [12] Soto-Abraham MV, Soriano-Rosas J, Díaz-Quiñónez A, et al. Navarro-Reynoso. Pathological changes associated with the 2009 H1N1 virus. *N Engl J Med* 2009;361(20):2001–3.
- [13] Korteweg C, Gu J. Pathology, molecular biology, and pathogenesis of avian influenza A (H5N1) infection in humans. *Am J Pathol* 2008;172(5):1155–70.
- [14] Ng WF, To KF, Lam WW, et al. The comparative pathology of severe acute respiratory syndrome and avian influenza A subtype H5N1—a review. *Hum Pathol* 2006;37(4):381–90.
- [15] Müller NL, Ooi GC, Khong PL, et al. Severe acute respiratory syndrome: radiographic and CT findings. *AJR* 2003;181(1):3–8.
- [16] Ajlan AM, Quiney B, Nicolaou S, et al. Swine-origin influenza A (H1N1) viral infection radiographic and CT findings. *AJR* 2009;193(6):1494–9.
- [17] Müller NL, Ooi GC, Khong PL, et al. High-resolution CT findings of severe acute respiratory syndrome at presentation and after admission. *AJR* 2004;182(1):39–44.

- [18] Kettil LH. Conventional wisdom: unconventional virus. *AJR* 2009;193(6):1486–7.
- [19] Kettil L, Paul N, Wong K. Radiology of severe acute respiratory syndrome (SARS): the emerging pathologic–radiologic correlates of an emerging disease. *J Thorac Imaging* 2006;21(4):276–83.
- [20] Lee N, Hui D, Wu A, et al. A major outbreak of severe acute respiratory syndrome in Hong Kong. *N Engl J Med* 2003;348(20):1986–94.
- [21] Remy-Jardin M, Giraud F, Remy J, et al. Importance of ground-glass attenuation in chronic diffuse infiltrative lung disease: pathologic–CT correlation. *Radiology* 1993;189(3):693–8.
- [22] John SD, Ramanathan J, Swischuk LE. Spectrum of clinical and radiographic findings in pediatric mycoplasma pneumonia. *RadioGraphics* 2001;21(1):121–31.
- [23] Davies A, Jones D, Bailey M, et al. Extracorporeal membrane oxygenation for 2009 influenza A (H1N1) acute respiratory distress syndrome. *JAMA* 2009;302(17):1888–95.